Influence of multi-impacts on GFRP composites laminates

A.M. Amaro, P.N.B. Reis, M.F.S.F. de Moura, M.A. Neto

PII: S1359-8368(13)00143-1
DOI: http://dx.doi.org/10.1016/j.compositesb.2013.03.041
Reference: JCOMB 2323

To appear in: *Composites: Part B*

Received Date: 27 November 2012
Revised Date: 12 March 2013
Accepted Date: 19 March 2013

Please cite this article as: Amaro, A.M., Reis, P.N.B., de Moura, M.F.S.F., Neto, M.A., Influence of multi-impacts on GFRP composites laminates, *Composites: Part B* (2013), doi: http://dx.doi.org/10.1016/j.compositesb.2013.03.041

Influence of multi-impacts on GFRP composites laminates

A.M.Amaro[1], P.N.B. Reis[2], M.F.S.F. de Moura[3], M. A. Neto[1]

[1] CEMUC; Department of Mechanical Engineering, University of Coimbra,

Pinhal de Marrocos, 3030 Coimbra, Portugal,

Tel.+351239790700; Fax +351239790701, ana.amaro@dem.uc.pt

[2] Department of Electromechanical Engineering, University of Beira Interior, 6200 Covilhã – Portugal

[3] Faculdade de Engenharia da Universidade do Porto, Rua Dr. Roberto Frias, 4200 Porto – Portugal

Abstract

The behaviour of Glass Fibre Reinforced Composites (GFRP) under single and multi-impact events of the same total energy was analysed. Experimental tests were performed considering circular simple supported plates impacted on its centre. The analyses of the results issuing from load-time, load-displacement and energy-time curves have shown that the sole impact of 3J is more detrimental for the plate, relative to the other cases of cumulative damage (1J+2J and 1J+1J+1J). A fine-tune analysis of damage evolution between subsequent impacts using a numerical procedure including a cohesive mixed-mode damage model was also performed. This analysis permits to verify the evolution of the projected delaminated area as well as the fracture process zone in the vicinity of delaminations. It was verified that a negligible evolution of damage occurs in the case of three consecutive impacts of the same energy. Additionally, it was concluded that the cumulative damage in the case of (1J+2 J) is inferior to the one propitiated by the sole impact of maximum energy (3 J).

Keywords: A. Polymer-matrix composites (PMCs); B. Impact behavior; C. Finite element analysis (FEA); D. Mechanical testing.

INTRODUCTION

Low velocity impact events can occur in-service or during the maintenance activities and can be considered one of the most dangerous loads on composite laminates. Different types of damages can occur like: matrix cracking, fibre fracture and fibre-matrix debonding [1]. However, delamination between different oriented layers is the predominant consequence of low velocity impact in composites [2]. The impact energy is generally absorbed by internal damage mechanisms resulting for the interaction of the several damage types without exterior signs detectable by visual inspection. Although adequate detection techniques can be used to quantify the severity of these damages [3, 4], low velocity impacts can be viewed as unsafe type of loads since they affect dramatically the performance of composites. Compressive strength, for example, is significantly affected by delaminations and is therefore considered to be a design limiting parameter [5]. Internal delaminations usually induce premature buckling of the structures with consequent drop of compressive strength [6-8]. In terms of tensile strength similar tendency is observed [9], although the respective strength is much less affected when compared with the compressive loading case. Effectively, Reis *et al* [9] observed reductions of ultimate strength around 16% in carbon/epoxy laminates while the drops in compressive strength can reach 60% [10-11]. The flexural properties of these materials are also affected by delaminations namely when damage is located close to the mid-thickness of the specimen [12, 13].

While the impact strength under single-impact loading is widely studied, the performance of composites under repeated impacts has attracted less attention although few works can be found in literature. Morais *et al* [14, 15], concluded that stacking sequences and laminate thickness are important parameters which influence the performance of composite structures under repeated impacts. From the experimental results they observed that the cross-ply and non-symmetric laminates have a better performance against low impact events than unidirectional laminates. For the unidirectional

laminates, trough thickness cracks can develop, leading to their fast failure [15]. On the other hand, the results obtained also show that below a certain energy level the cross section of the laminate is the most relevant variable that determines the impact resistance [14]. Cholakara *et al* [16] studied the effect of repeated impacts and observed that stitched Kevlar-fibre/epoxy composites were able to withstand more impacts than the non-stitched laminate before failing. Mouritz *et al* [17] observed that stitched glass reinforced laminates suffered severe microstructural damage under repeated impacts, including shear cracking of the resin, delaminations, crushing and fracture of the glass fibres. These authors concluded that composites under single-impact loading suffer a slight reduction in flexural strength but a large reduction in interlaminar shear strength. The shear strength is reduced considerably because a single impact creates the main types of damage necessary for shear failure, i.e. shear-induced polymer cracking, debonding and delaminations. However, under repeated impacts the laminates experienced a large deterioration in flexural strength because of fracture of the glass fibres [17]. Wyrick and Adams [18] observed that damage in the carbon/epoxy laminates increased with increasing number of impacts of the same energy. The main damage occurs during the first impact and, after, each impact promotes little incremental damages [18]. On the other hand, Ho *et al* [19] shows that the fibre pullout and fibre breakage are the major fracture mechanisms in repeated impacts for polycarbonate composites. Studies developed by Hosur *et al* [20] show that at lower energy levels the peak load does not change significantly with number of impacts but at higher energy levels there is sudden drop in peak load after certain number of impacts. Absorbed energy also showed similar trend with respect to number of impacts. Damage area increases with number of impacts, but after certain number of impacts it does not increase significantly [20]. Experimental tests developed by Icten [21] on Glass/Epoxy composites show that, except for the first three impacts, the maximum contact force decreases and energy absorbed by the composite increases with the impact number. At same time, the laminates impacted at low

temperature (-40ºC) reveal higher peak force and lower absorbed energy than that impacted at room temperature. Therefore, the low temperature increases the number of impacts to failure.

To the authors' knowledge, studies of multi-impacts with sequences of different energy levels were not yet performed. Then, the aim of this work is to verify the influence of repeated low velocity impact with different energy levels on glass fibre epoxy laminates. For this purpose different energies were combined in the following sequences 3 J, (1+2) J and (1+1+1) J in order to understand the effect of multi-impacts, combined with different energy values but with the same total amount of one single impact of 3 J. Experimental tests and numerical simulations were performed. The numerical approach is based on a three-dimensional analysis including a cohesive mixed-mode (I+I+III) damage model implemented via interface finite elements [22]. The objective of the numerical analysis is to understand the different damage evolutions between the three studied cases. The analysis of the experimental and numerical results provided fruitful conclusions about the effect of multi-impacts combined with different energy values compared with a single impact.

2. MATERIALS AND PROCEDURE

Composite laminates were prepared in the laboratory from glass fibre Prepreg TEXIPREG® ET443 (EE190 ET443 Glass Fabric PREPREG from SEAL, Legnano, Italy) and processed in agreement with the manufacturer recommendations. The volume fraction of E glass fibre is 0.45 and the laminates were processed using the autoclave/vacuum-bag moulding process. The processing setup consisted of several steps: make the hermetic bag and apply 0.05 MPa vacuum; heat up to 125º C at a 3-5º C/min rate; apply a pressure of 0.5 MPa when a temperature of 120-125º C is reached; maintaining pressure and temperature for 60 min; cool down to room temperature maintaining pressure and finally

get the part out from the mould. The laminates were manufactured with the stacking sequence $[45_2, 90_2, -45_2, 0_2]_s$.The unidirectional mechanical properties are listed in Table 1. The plates were manufactured in a useful size of 300 x 300 x 2.6 mm^3.

The specimens used in the experiments were cut from these thin plates, using a diamond saw and a moving speed chosen to reduce the heat in the specimen. The low velocity impact tests were performed using a drop weight-testing machine Instron-Ceast 9340 and a 10 mm impactor diameter with a mass of 3.4 kg was used. The tests were performed on circular samples of 70 mm diameter and the impactor stroke at the centre of the samples obtained by centrally supporting the 100x100 mm specimens. The impact energies used were 3 J, 2 J and 1 J, however, they were combined in the following sequences 3 J, (1+2) J and (1+1+1) J in order to understand the effect of multi-impacts, combined with different energy values but with the same total value of one single impact (3 J). For each condition, five specimens were tested at room temperature. After impact tests, all the specimens were inspected in order to evaluate the size and shape of the delaminations. As the glass-laminated plates are translucent it is possible to obtain an image of the damage using photography. To achieve the best possible definition of the damaged area, the plates were photographed in counter-light using a powerful light source. Plates were framed in a window so that all the light could fall upon them.

3. NUMERICAL ANALYSIS

A numerical analysis based on finite element method was also performed in order to better understand the phenomena that explain the observed experimental behaviour. A three-dimensional analysis including cohesive zone modelling was used to simulate delaminations and fracture process zones at interfaces between different oriented layers [22]. The cohesive mixed-mode (I+II+III) damage

model is based on a quadratic stress criterion to simulate damage initiation

$$\left(\frac{\sigma_{\mathrm{I}}}{\sigma_{\mathrm{u,I}}}\right)^2+\left(\frac{\sigma_{\mathrm{II}}}{\sigma_{\mathrm{u,II}}}\right)^2+\left(\frac{\sigma_{\mathrm{III}}}{\sigma_{\mathrm{u,III}}}\right)^2=1 \quad \text{if} \quad \sigma_{\mathrm{I}}\geq 0$$
$$\left(\frac{\sigma_{\mathrm{II}}}{\sigma_{\mathrm{u,II}}}\right)^2+\left(\frac{\sigma_{\mathrm{III}}}{\sigma_{\mathrm{u,III}}}\right)^2=1 \quad \text{if} \quad \sigma_{\mathrm{I}}\leq 0 \qquad (1)$$

where σ_i (i = I, II, III) represent the stress components in each loading mode and $\sigma_{\mathrm{u},i}$, (i=I, II, III) are the local strengths. When the above criterion is satisfied, a linear softening relationship between stresses and relative displacements is assumed at the integration points (Figure 1). The definition of the ultimate relative displacement corresponding to complete failure is realized through the linear energetic criterion

$$\frac{G_{\mathrm{I}}}{G_{\mathrm{Ic}}}+\frac{G_{\mathrm{II}}}{G_{\mathrm{IIc}}}+\frac{G_{\mathrm{III}}}{G_{\mathrm{IIIc}}}=1 \qquad (2)$$

where G_i (i = I, II, III) are the strain energy components and G_{ic} the respective critical values. When this criterion is satisfied at a given integration point total failure occurs, thus simulating delamination growth. Shear and normal tensile stresses vanish at the integration point, being only able to transmit normal compressive stresses. The cohesive damage model is implemented on Abaqus software by means of the User Subroutine tool. More details about the used model are presented in [22].

One aspect that deserved special attention was the modelling of the quasi-isotropic stacking sequence of the laminate $[45_2,90_2,-45_2,0_2]_s$. This laminate is constituted by seven groups of equally oriented layers which means that delaminations can arise at six interfaces. In a three-dimensional numerical analysis it would be necessary to consider seven layers of solids elements separated by six layers of cohesive elements. However, it is known that delaminations are inexistent or very small at "upper" interfaces, i.e., at interfaces proximal to impacted surface, due to influence of the normal

compressive stresses [22]. Consequently, the ten upper layers of the laminate were homogenised considering the classical laminate theory to get the global elastic properties. In this context, only four layers of solid elements modelling each group of equally oriented layers ([45_2,90_2,-45_2,Homogeneised]), and three layers of cohesive elements between those layers were considered in the problem to simplify the analysis and diminish the time computation. A total number of 2304 three-dimensional 8-node isoparametric solid elements (576 per layer) and 1728 8-node cohesive elements (576 per interface between different oriented layers) were considered. A quasi-static non-geometrical analysis was performed considering very small increments to avoid numerical instabilities. The quasi-static analysis is justified by the fact that contact between the impactor and the plate in a low velocity impact is a sufficiently long event to give rise to an equilibrium condition [23]. The impactor was simulated as a rigid body and contact conditions between it and the specimen were imposed to avoid interpenetrations (see Figure 2).

4. RESULTS AND DISCUSSION

4.1. Experimental results

Figure 3 shows typical load-time curves and Figure 4 presents the typical load-displacement curves. These diagrams represent a typical behaviour and are in agreement with those reported in literature [24-27]. It is possible to observe, that the load increases up to a maximum value (P_{max}) followed by a drop corresponding to the impactor rebound. As expected the values of maximum load and maximum displacement increase with increasing impact energy (Figure 4 and Table 2). In this figure it can be observed that the area circumscribed between the loading and unloading branches increases with the impact energy thus reflecting larger energy dissipation, which obviously is a

symptom of larger internal damage in the specimen. Figure 4c revels that for the same energy level the multi-impacts lead to slightly increase of displacement and decrease of maximum load as a consequence of damage accumulation. However, the energy dissipation in each of the three tests is similar (Table 2). Figure 5 represents typical energy versus time curves. The beginning of the plateau of the curve corresponds to contact loss between the impactor and the specimen [26-28]. The difference between the maximum energy corresponding to maximum plate deflection and the energy defined by the plateau is the restitution component due to impactor rebound. From Figures 5a-c and Table 2, it can be seen that higher impact energies present lower energy restitution and, consequently, major energy dissipated by the specimen thus confirming the statements issuing from Figure 4.

As the glass-laminated plates are translucent it is possible to get the image revealing the damage envelop. For this purpose the plates were photographed on the opposite side of the impact (back face) and a typical picture is shown in Figure 6. This image corresponds to the superposition of delaminations located at several interfaces between different oriented layers. Anyway, it can be concluded that the major delamination occurs at the lowest interface (between 90º and 45º groups of layers), and is oriented on the fibres direction of the adjacent lower ply, i.e., 45º (it should be noted that photographs were taken on the non-impacted surface and are, consequently, rotated). A longitudinal crack aligned with the fibres direction of this lowest ply is also visible and constitutes the initial damage induced by bending [29]. This crack leads to a delamination along the upper adjacent interface, thus revealing a complex damage mechanism based on interaction between matrix cracking and delamination. This damage mechanism also occur for the nearer layers and interfaces between different oriented layers in a minor scale. This visual inspection in counter-light allows a rough estimation of the damage area. Nevertheless, it can be observed that the single impact of 3 J induces the largest damaged area (around 505 mm^2), followed by the (1+2) J case (around 480 mm^2) and (1+1+1) J which presents

the least damaged plate (around 225 mm^2). Then, the (1+1+1) J and (1+2) J sequences promote lower damages than a single impact of 3 J. This result is coherent with the statements about energy dissipation that emerged from the analysis of Figures 4 and 5.

4.2. Numerical results

The numerical analysis was performed in order to understand the details of delamination development in each of the three analyzed cases considering the properties listed in Table 1. Cohesive elements allow simulating delaminations at the three considered interfaces between different oriented layers. Two damage states can be analysed at each integration point: a completely delaminated point occurs when the energetic criterion (equation (2)) is satisfied; a point that is undergoing damage (equation (1) is satisfied), but did not completely failed, i.e., a point that is located on the descending branch of the softening law (Figure 1). This last type of points simulates the fracture process zone (FPZ), which is a region located in the vicinity of the crack tip where several inelastic processes (e.g., micro-cracking, plastification) take place. Consequently, the profile of delaminations and the corresponding FPZ at a given increment can be obtained from the coordinates of the integration points whose failure condition is dictated by the statements described above. This analysis allows monitoring the evolution of delaminations and FPZ in the multi-impacts cases. In fact, the damage resulting for a given impact is registered in a file containing the state of the damage variables in each integration point at the maximum load listed in Table 2. In the next impact event the referred file is inputted in the model thus simulating a pre-damaged plate. The objective is analyzing in detail the evolution of delaminations and FPZ between consecutives impacts and revealing the effect of cumulative damage. This fine-tune analysis is not possible experimentally since the image produced by counter-light observation does not allow to clearly distinguish delamination from the FPZ around it.

Figure 7 shows the typical profile obtained for the numerical and experimental load-displacement curves. Numerically, the damage is registered for each case considering the average maximum load listed in Table 1. Figures 8a-c present the damage evolution between the three consecutive tests considering impact energy of 1 J. A slight increase of the FPZ between the first and the second impact can be observed, but no increase of damage takes place between the second and third impacts thus revealing a stabilization process for this level of energy. Generally, it can be concluded that damage induced by the first impact practically does not alter in result of the subsequent events. This conclusion is in agreement with the typical profiles of the load-displacement curves (Figure 4) which revealed slight variation between the three impacts. Figures 8d-e highlight a clear evolution of damage between the first impact event of 1 J and the second one with an energy of 2 J. Even though, the cumulative damage issuing from these two events is even inferior to damage resulting from a sole impact of 3 J (Figure 8f).

5. CONCLUSIONS

Multi-impact behaviour of glass/epoxy laminated composites with a quasi-isotropic layup was analysed. Three different sequences of impacts adding up the same global energy ((1+1+1) J, (1+2) J and 3 J) were used in order to compare the resulting damage. The projected damaged area was estimated by observation in counter-light using a powerful light source owing to the plate's translucency. It was observed that damage increases with the value of the higher impact event in each sequence, i.e., a sole impact of 3 J is more detrimental relative to cumulative damage issued form multi-impact events. This observation was also confirmed by the evolution of load-time, load-displacement and energy-time curves which have shown that energy dissipated by damage

development increases with the value of impact energy.

A three-dimensional numerical analysis considering cohesive mixed-mode I+II+III damage model was also performed in order to better understand the details of damage development in the considered sequences of impact events. The numerical results have shown that damage maintains practically constant for the sequence of three impacts of 1 J. The same does not happen for the 1+2 J sequence of impacts, although the resulting cumulative damage is still inferior to the case of a unique 3 J impact event.

REFERENCES

[1] Richardson MOW, Wisheart MJ. Review of low-velocity impact properties of composite materials. Compos Part A-Appl S 1996; 27: 1123-1131.

[2] Abrate S. Impact on laminated composite materials. Appl Mech Rev 1991; 44: 155–190.

[3] Adams RD, Cawley PD. A Review of Defects Types and Non-Destructive Testing Techniques for Composites and Bonded Joints. NDT Int 1998; 21: 208-222.

[4] Amaro AM, Reis PNB, de Moura MFSF, Santos JB. Damage Detection on Laminated Composite Materials Using Several NDT Techniques. Insight 2012; 54: 14-20.

[5] Goutianos S, Galiotis C, Peijs T. Compressive Failure Mechanisms in Multi-fibre Microcomposites. Compos Part A-Appl S 2004; 35: 461-475.

[6] Nakanishi Y, Hana K, Hamada H. Fractography of Fracture in CFRP under Compressive Load. Compos Sci Technol 1997; 57: 1139-1147.

[7] Lankford J. Shear versus Dilatational Damage Mechanisms in the Compressive Failure of Fibre-reinforced Composites. Compos Part A-Appl S 1997; 28: 215-222.

[8] Lee SH, Yerramalli CS, Waas AM. Compressive Splitting Response of Glass–fiber Reinforced Unidirectional Composites. Compos Sci Technol 2000; 60: 2957-2966.

[9] Reis PNB, Ferreira JAM, Antunes FV, Richardson MOW. Effect of Interlayer Dalamination on Mechanical Behavior of Carbon/Epoxy Laminates. J Compos Mater 2009; 43: 2609-2621.

[10] Davies GAO, Hitchings D, Zhou G. Impact Damage and Residual Strengths of Woven Fabric Glass/Polyester Laminates. Compos. Part A-Appl S 1996; 27: 1147-1156.

[11] de Moura MFSF, Marques AT. Prediction of Low Velocity Impact Damage in Carbon-Epoxy Laminates. Compos. Part A-Appl S 2002; 33: 361-368.

[12] Amaro AM, de Moura MFSF, Reis PNB. Residual Strength After Low Velocity Impact in Carbon-Epoxy Laminates. Mater Sci Forum 2006; 514-516: 624-628.

[13] Amaro AM, Reis PNB, de Moura MFSF. Delamination Effect on Bending Behaviour in Carbon–Epoxy Composites. Strain 2011; 47: 203-208.

[14] de Morais WA, Monteiro SN, d'Almeida JRM. Effect of the Laminate Thickness on the Composite Strength to Repeated Low Energy Impacts. Compos Struct 2005; 70: 223–228.

[15] de Morais WA, Monteiro SN, d'Almeida JRM. Evaluation of Repeated Low Energy Impact Damage in Carbon-epoxy Composite Materials. Compos Struct 2005; 67: 307-315.

[16] Cholakara MT, Jang BZ, Wang CZ. Deformation and Failure Mechanisms in 3D Composites. In Proc. 34th Int. SAMPE Conference, May 8-11, 2153-2160, 1989.

[17] Mouritz AP, Gallagher J, Goodwin AA. Flexural Strength and Interlaminar Shear Strength of Stitched GRP Laminates Following Repeated Impacts. Compos Sci Technol 1997; 57: 509-522.

[18] Wyrick DA, Adams DF. Damage Sustained by a Carbon/epoxy Composite Material Subjected to Repeated Impact. Composites 1988; 19: 19-26.

[19] Ho KC, Hwang JR, Doong JL. Impact Fatigue of Short Glass Fiber Reinforced Polycarbonate. J Reinf Plast Compos 1997; 16: 903-925.

[20] Hosur MV, Karim MR, Jeelani S. Experimental Investigations on the Response of Stitched/unstitched Woven S2-glass/SC15 Epoxy Composites Under Single and Repeated Low Velocity Impact Loading. Compos Struct 2003; 61: 89-102.

[21] Icten BM. Repeated Impact Behavior of Glass/Epoxy Laminates. Polym Composite 2009; 30: 1562-1569.

[22] Durão LMP, de Moura MFSF, Marques AT. Numerical simulation of the drilling process on carbon/epoxy composite laminates. Compos Part A-Appl S 2006; 37: 1325–1333.

[23] de Moura MFSF, Marques AT. Prediction of Low Velocity Impact Damage in Carbon-Epoxy Laminates. Compos Part A-Appl S 2002;33:361-368.

[24] Hosur MV, Adbullah M, Jeelani S. Studies on the low-velocity impact response of woven hybrid composites. Compos Struct 2005; 67: 253-262.

[25] Iqbal K, Khan S-U, Munir A, Kim J-K. Impact damage resistance of CFRP with nanoclay-filled epoxy matrix. Compos Sci Technol 2009; 69: 1949-1957.

[26] Reis PNB, Ferreira JAM, Santos P, Richardson MOW, Santos JB. Impact Response of Kevlar composites with filled epoxy matrix. Compos Struct 2012; 94: 3520-3528.

[27] Reis PNB, Ferreira JAM, Zhang ZY, Benameur T, Richardson MOW. Impact Response of Kevlar Composites with Nanoclay Enhanced Epoxy Matrix. Compos Part B-Eng doi: 10.1016/j.compositesb.2012.10.028.

[28] Río TG, Zaer R, Barbero E, Navarro C. Damage in CFRPs due to low velocity impact at low temperature. Compos Part B-Eng 2005; 36: 41-50.

[29] de Moura MFSF, Gonçalves JPM. Modelling the Interaction between Matrix Cracking and Delamination in Carbon-epoxy Laminates under Low Velocity Impact. Compos Sci Technol 2004; 64: 1021-1027

TABLES

Table 1 – Mechanical properties of unidirectional glass/epoxy composite.

E_1 [GPa]	$E_2 = E_3$ [GPa]	$\nu_{12} = \nu_{13}$	ν_{23}	$G_{12} = G_{13}$ [GPa]	G_{23} [GPa]	G_{Ic} [N/mm]	$G_{IIc}=G_{IIIc}$ [N/mm]	$\sigma_{u,I} = \sigma_{u,II}$ [MPa]
50	10	0.34	0.38	3.0	2.79	0.15	0.3	20

Table 2 – Experimental results for laminates impacted with single and multi-impacts.

	Impact sequences					
	3 J	(1+2) J		(1+1+1) J		
		1 J	2 J	1 J	1 J	1 J
Maximum load [kN]	1.55 (4.1)	1.08 (3.7)	1.49 (5.3)	1.09 (3.5)	1.07 (4.9)	1.04 (6.4)
Maximum displacement [mm]	4.1 (2.7)	2.52 (2.1)	3.23 (3.8)	2.49 (2.4)	2.62 (4.1)	2.8 (5.2)
Contact time [ms]	11.9 (4.8)	10.3 (3.9)	11.5 (4.5)	10.3 (4.1)	10.7 (5.3)	11.2 (6.1)
Restitution energy [%]	27 (3.9)	78.6 (3.5)	40.9 (5.6)	78.7 (3.8)	76.9 (5.7)	72.5 (7.3)

( ) is the standard deviation in %.

FIGURES

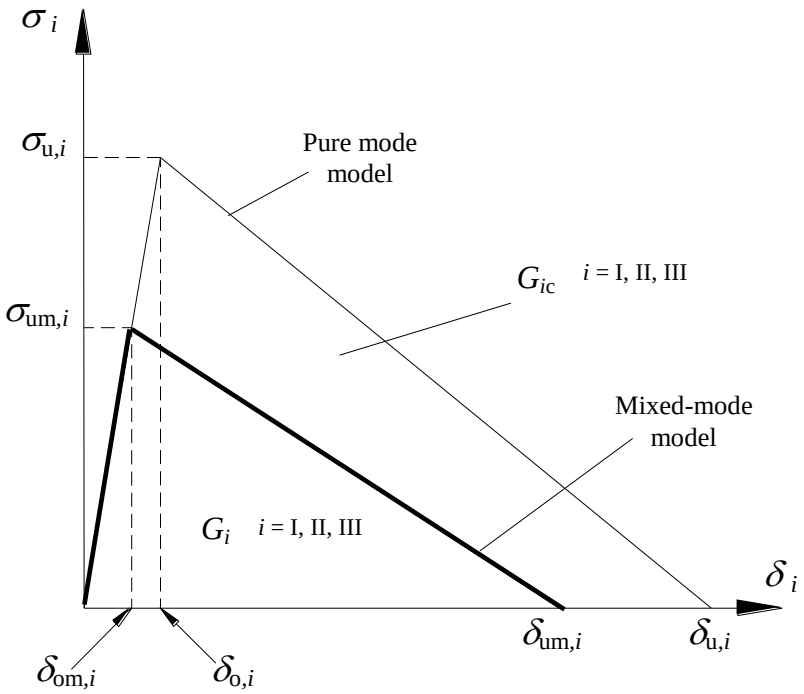

Figure 1 – The triangular softening law for pure mode and mixed mode; σ-stress; δ-displacement; G-strain energy release rate; G_c-fracture energy; subscripts (m-Mixed-mode; u-ultimate; o-onset; i-loading mode).

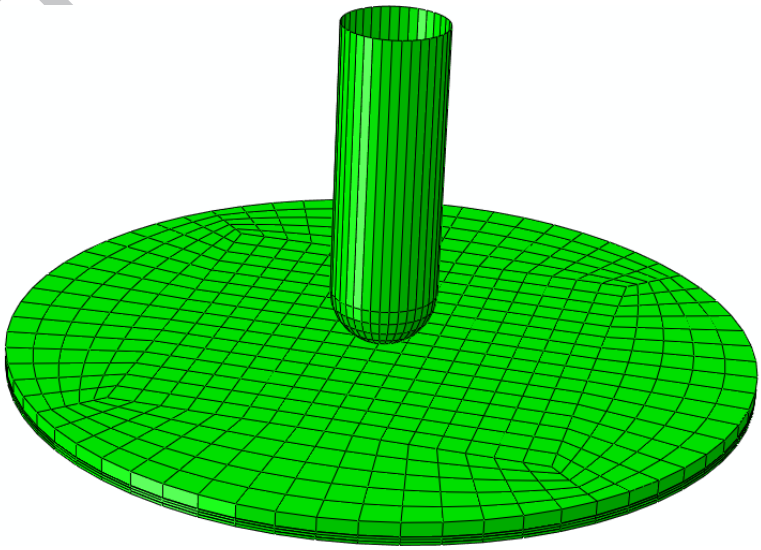

Figure 2 – Simulation of impact on supported circular plates.

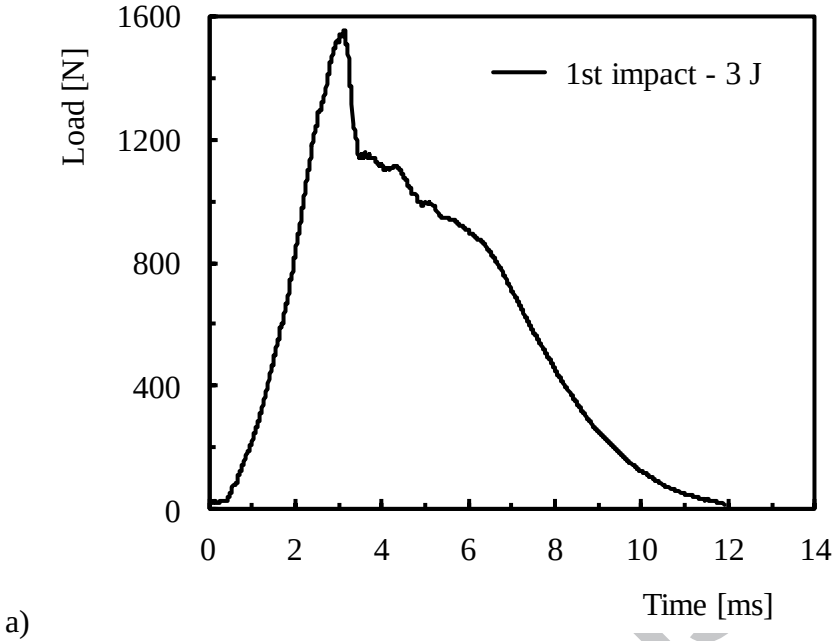

a)

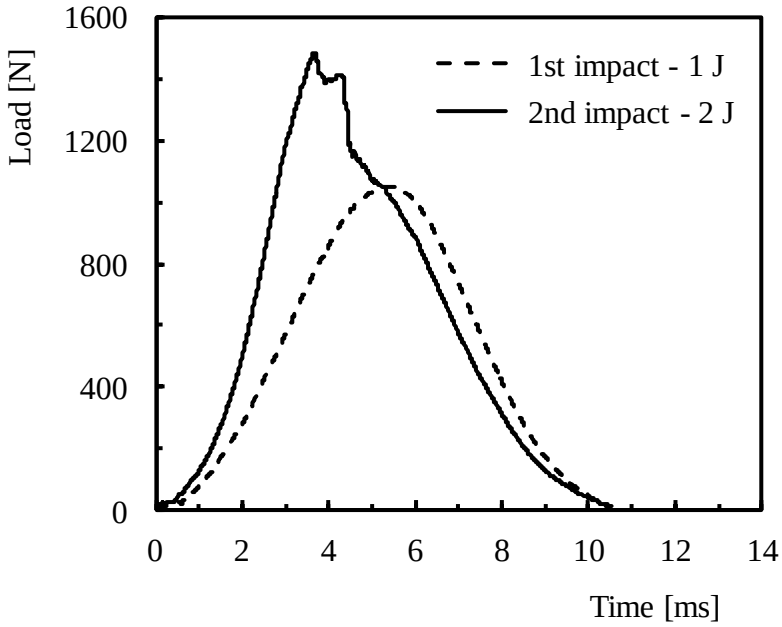

b)

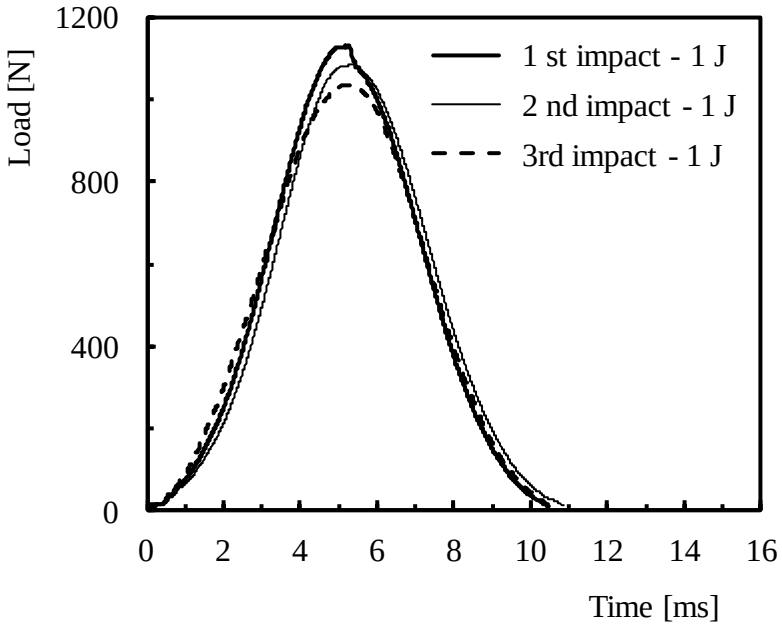

c)

Figure 3 – Typical load versus time curves for: a) 3 J; b) Sequence (1+2) J; c) Sequence (1+1+1) J.

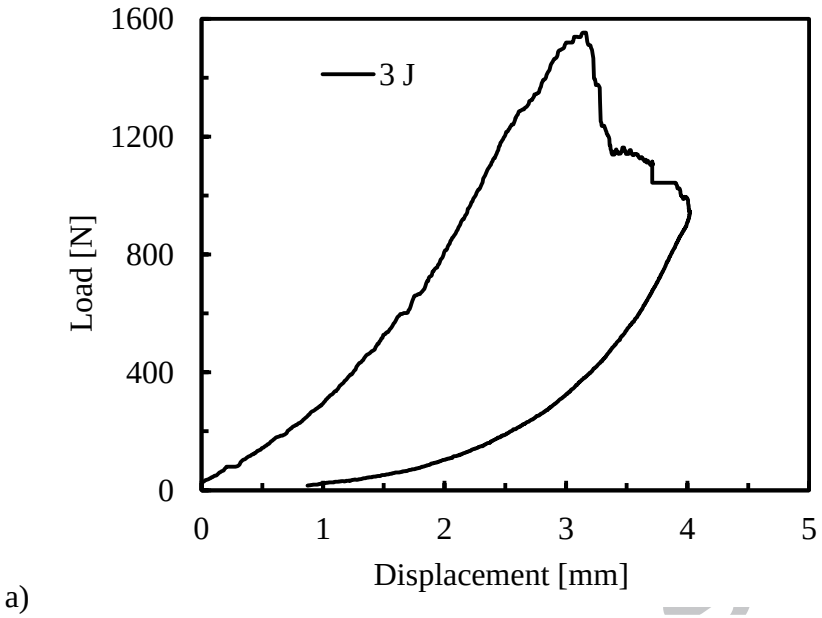

a)

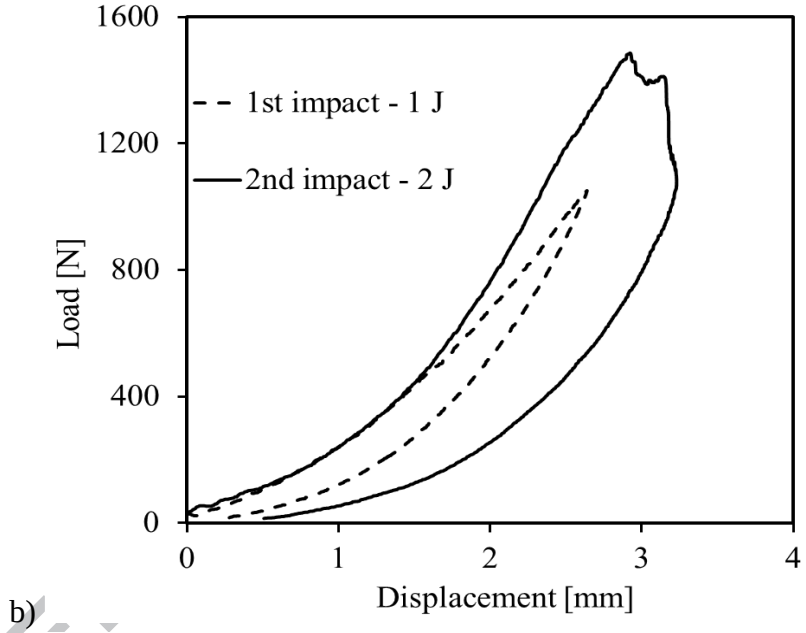

b)

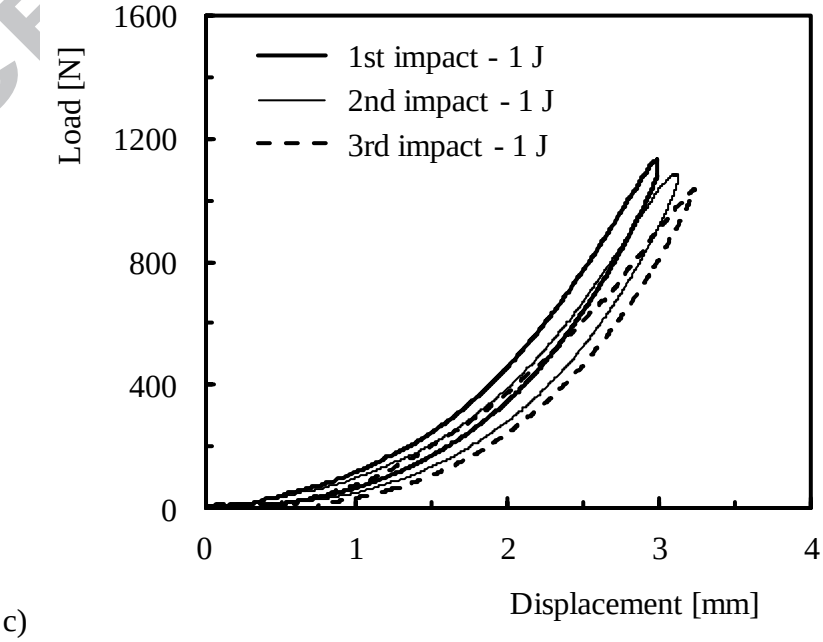

c)

Figure 4 – Typical load versus displacement curves for: a) 3 J; b) Sequence (1+2) J; c) Sequence (1+1+1) J.

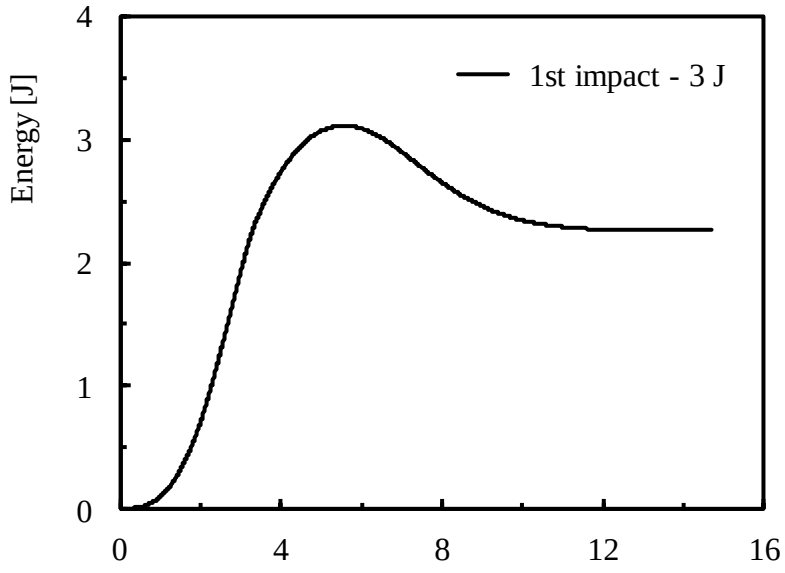

a)

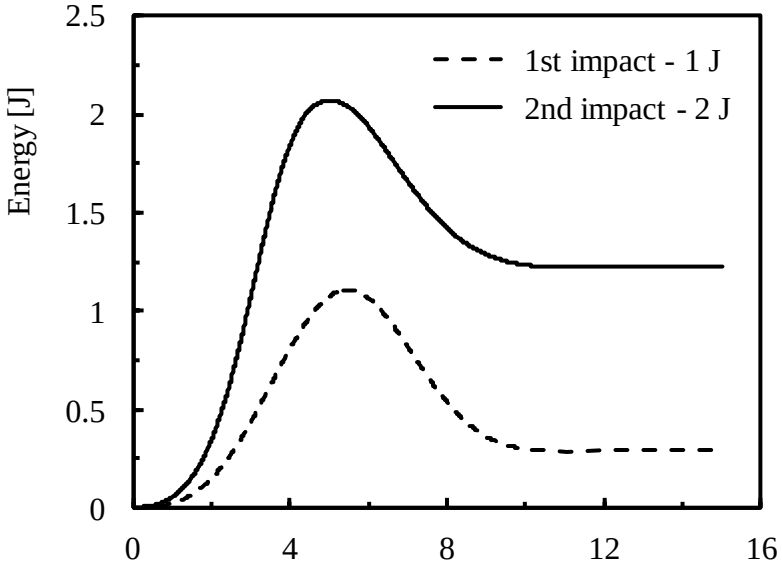

b)

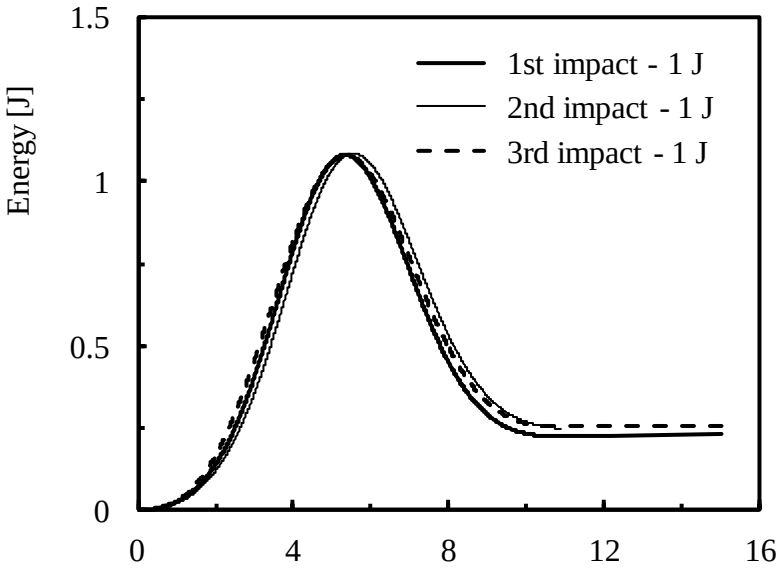

c)

Figure 5 – Typical energy versus time curves for: a) 3 J; b) Sequence (1+2) J; c) Sequence (1+1+1) J.

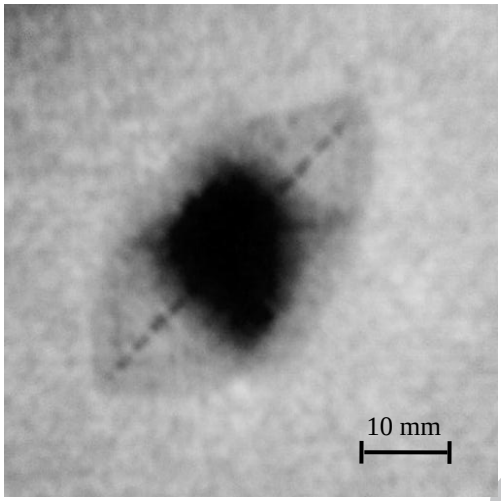

Figure 6 - Typical damages occurred for all laminates (the picture shows the damage after impact at 3 J).

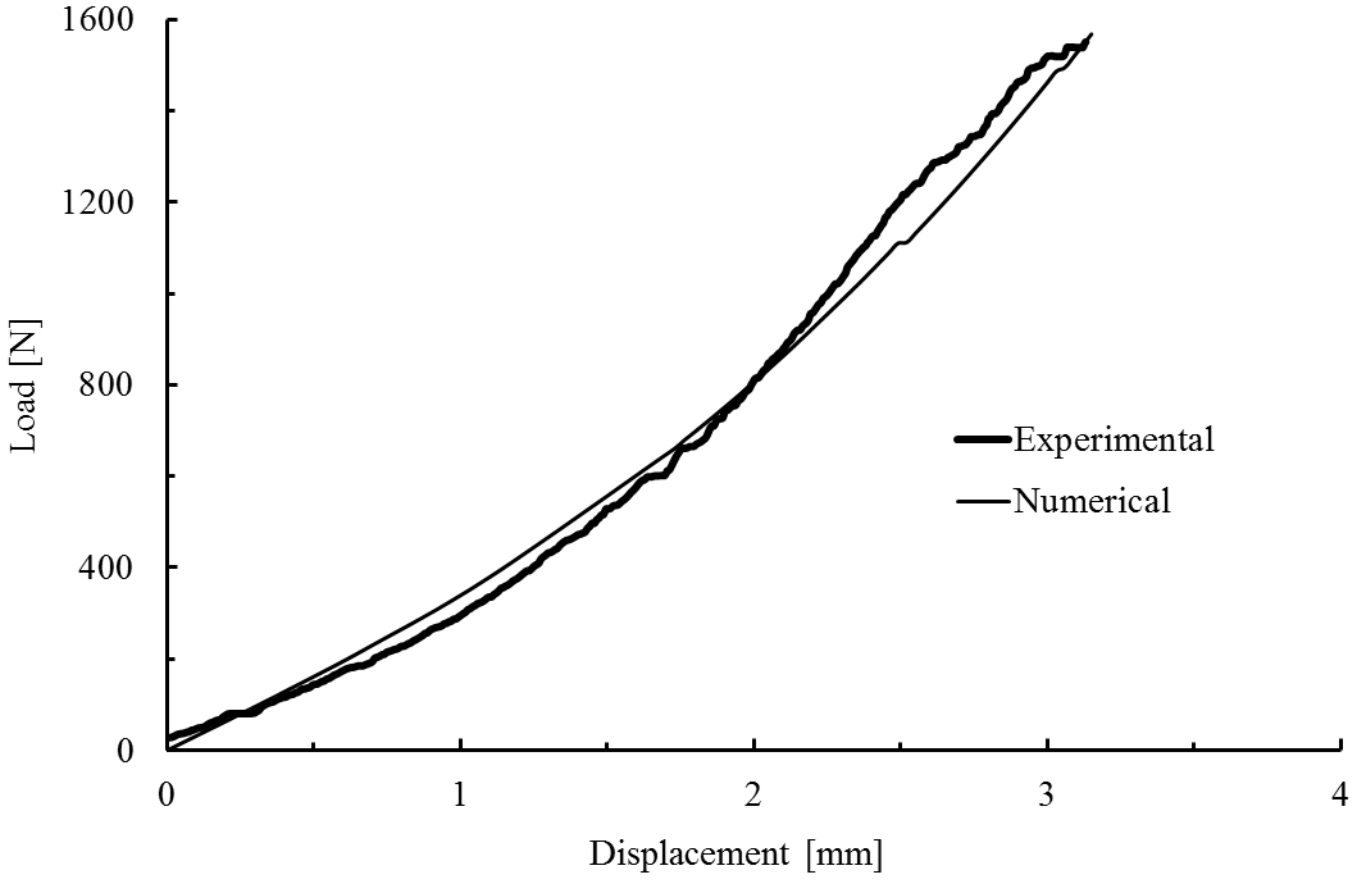

Figure 7 – Load-displacement curves for the 3 J impact.

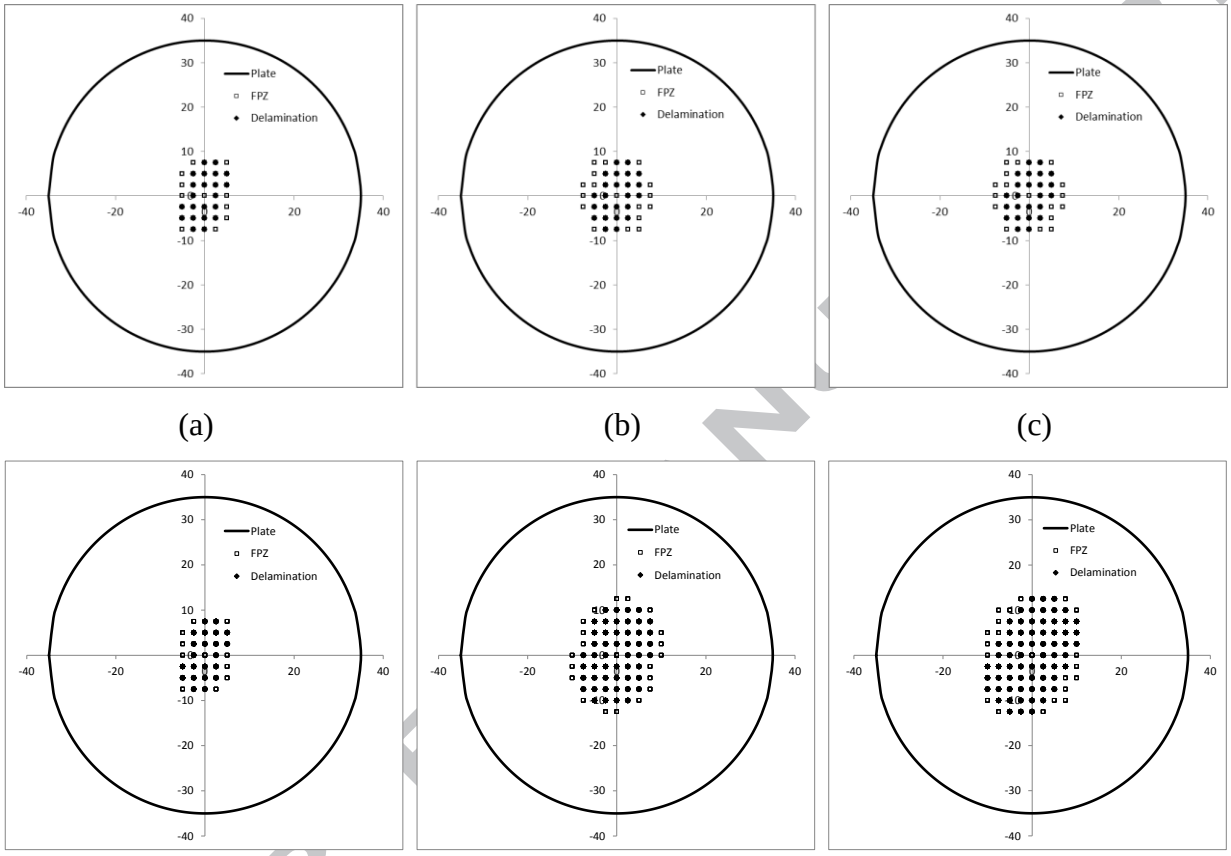

Figure 8 – Damage development (dimensions in mm) for the several impact events: (a) First impact of 1 J; (b) Second impact of 1 J; (c) Third impact of 1 J; (d) First impact of 1 J; (e) Second impact of 2 J; (f) Impact of 3 J.